PHYSICAL REVIEW B **80**, 140201(R) (2009)

$Fe_{23}B_6$-type quasicrystal-like structures without icosahedral atomic arrangement in an Fe-based metallic glass

Akihiko Hirata,[1,*] Yoshihiko Hirotsu,[2] Kenji Amiya,[3] Nobuyuki Nishiyama,[4] and Akihisa Inoue[1]
[1]*WPI Advanced Institute for Materials Research, Tohoku University, Sendai 980-8577, Japan*
[2]*R&D Institute of Metals and Composites for Future Industries (RIMCOF), Osaka University Laboratory, Osaka 567-0047, Japan*
[3]*Institute for Materials Research, Tohoku University, Sendai 980-8577, Japan*
[4]*R&D Institute of Metals and Composites for Future Industries (RIMCOF), Tohoku University Laboratory, Sendai 980-8577, Japan*
(Received 29 July 2009; published 29 October 2009)

We have found nanoscale quasicrystal-like structural states exhibiting pseudotenfold nanobeam electron-diffraction patterns in the course of nanocrystallization process of an $Fe_{23}B_6$ structure in an $(Fe_{0.5}Co_{0.5})_{72}B_{20}Si_4Nb_4$ metallic glass. An existence of the intermediate states between the quasicrystal-like and $Fe_{23}B_6$ structures indicates that the quasicrystal-like structure is approximate to the $Fe_{23}B_6$ structure including no icosahedral atomic arrangement. The pseudotenfold electron-diffraction patterns are understood from a combination of three types of tiles found in the $Fe_{23}B_6$ structure. The three types of tiles can produce decagonal units which do not have any icosahedral atomic arrangement.

DOI: 10.1103/PhysRevB.80.140201 PACS number(s): 64.70.pe, 61.05.jm, 64.70.dg

It has been well established that atomic structures of metallic glasses organized from some characteristic local atomic structures, such as icosahedral, prism, bcc-like, fcc-like, and other atomic polyhedral clusters.[1–4] The icosahedral atomic cluster has been paid special attention among the atomic clusters because its formation was predicted from liquid states of metallic glasses, and its symmetry is not compatible with a translational symmetry in crystals.[5] In a monoatomic Lennard-Jones system, the icosahedral cluster was found to have a lower energy than crystalline clusters.[5,6] Although realistic metallic glasses comprise multicomponent atoms with different atomic sizes, an existence of icosahedral(-like) atomic ordering has been reported for metal-metal type metallic glasses by many researchers.[7–10]

Especially in Zr-based metallic glasses, an icosahedral atomic arrangement is known as a basic structural unit of Ti_2Ni-type (big-cube) phase which is formed during the first crystallization process.[11–17] In addition, Li and Inoue pointed out that the Ti_2Ni-type structure can be regarded as a crystalline approximant of the icosahedral quasicrystal.[17] A concept of "crystalline approximant" was introduced for Al-based icosahedral quasicrystals to understand structural details of quasicrystal structures.[18] This is because that atomic positions can be accurately determined only for crystalline structures by using experimental diffraction techniques. According to the concept, we can find the crystal structure called "crystalline approximant" that is close to the quasicrystal structure based on the characteristic zone-axis diffraction patterns. In a case of the Zr-based metallic glasses, icosahedral atomic clusters, which are found in the Ti_2Ni-type structure, are expected to be formed in the quasicrystal structure and its icosahedral local atomic ordering is well consistent with the predictions for the glass structures by a large number of experimental and theoretical studies. Although this perspective seems reasonable and acceptable, direct experimental evidences are necessary to understand the structural linkage among glass, quasicrystal, and crystalline approximant structures.

In the metal-metalloid type metallic glasses, on the other hand, the trigonal prism structures with central metalloid atoms were found to be dominant[19,20] in a relatively high concentration range of the metalloid elements.[20,21] Considering this fact, it is unlikely that the quasicrystal structure is found to exist in metal-metalloid type metallic glasses. Recently, however, we have found quasicrystal-like structures in the course of nanocrystallization in the $Fe_{48}Cr_{15}Mo_{14}C_{15}B_6Tm_2$ bulk metallic glass (BMG),[22,23] although the structure has imperfect quasiperiodicity compared with the quasicrystal already found in many metal-metal type metallic glasses. In addition, we have also presented three structural states of quasicrystal-like structure, χ-FeCrMo (cI58 α-Mn-type) crystalline approximant, and intermediate structure between them, in the same alloy. The appearance of the quasicrystal-like structure is considered to be reasonable because of the structural similarity between the quasicrystal structure and the crystalline approximant with respect to the structural units with icosahedral atomic arrangements. Very recently, in an $(Fe_{0.5}Co_{0.5})_{72}B_{20}Si_4Nb_4$ BMG, we have also found quasicrystal-like structures, which are similar to the $Fe_{23}B_6$ structure (cF116 $Cr_{23}C_6$-type) with no icosahedral atomic cluster, in an $(Fe_{0.5}Co_{0.5})_{72}B_{20}Si_4Nb_4$ BMG. In this Rapid Communication, we report the structural features of the quasicrystal-like structures examined by using nanobeam electron-diffraction (NBED) technique. An origin for the pseudotenfold diffraction patterns is also discussed based on the $Fe_{23}B_6$ structure.

A ribbon of $(Fe_{0.5}Co_{0.5})_{72}B_{20}Si_4Nb_4$ metallic glass[24] was made by single-roll rapid quenching. The ribbon was about 0.8 mm in width and 20 μm in thickness. In order to observe the nanocrystallized microstructure by transmission electron microscopy (TEM), the ribbon specimens were annealed isothermally at 873K for 1 h in a vacuum furnace. Specimens for TEM observation were prepared by electropolishing (acetic-perchloric acid) at room temperature. The specimens were finally prepared by using an ion milling (GATAN PIPS) with a low voltage of 2.5 kV and a glancing angle of 4 deg. Selected area electron-diffraction (SAED) patterns and dark-field images were taken by 200 kV TEM

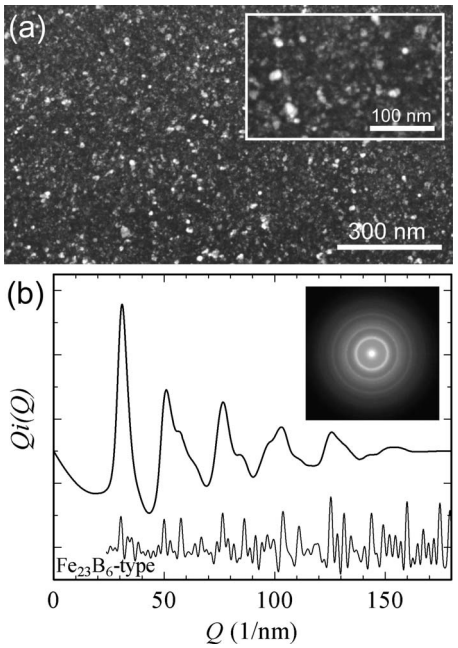

FIG. 1. (a) An energy-filtered dark filed image and (b) a reduced interference function $Qi(Q)$ profile obtained from the specimen annealed at 873K for 1 h. The dark-field image was taken by using a part of the first halo ring and the enlarged image is also shown in the inset of (a). A SAED pattern used in making the $Qi(Q)$ profile is also shown in the inset of (b).

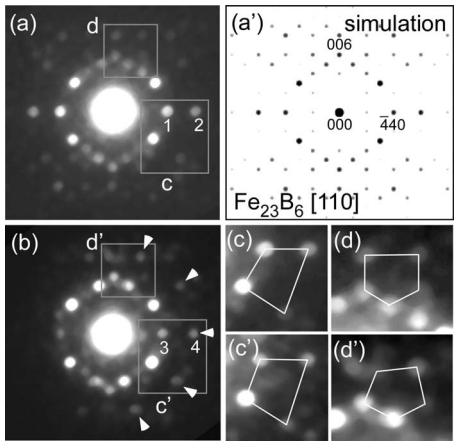

FIG. 2. Two types of NBED patterns, (a) perfect $Fe_{23}B_6$ and (b) $Fe_{23}B_6$-like patterns, obtained from the specimen annealed at 873K for 1 h. The electron incidence is parallel to the [110] direction of the $Fe_{23}B_6$ structure. The simulated diffraction pattern is also shown in (a′). For comparison, the surrounded areas in the patterns of (a) and (b) are enlarged in (c), (d), (c′), and (d′), respectively.

(LEO-922D) equipped with an omega-type energy filter. NBED patterns were obtained by 300 kV TEM (JEM-3000F). The amount of electron dose for the nanoprobe in NBED was 2.0×10^{19} e/cm^2 (measured by a Faraday gauge), almost ten times smaller than that for the conventional high-resolution electron microscope imaging. The SAED patterns and images were recorded on imaging plates (IP) and read using IP readers. The NBED patterns were recorded using a TV-rate camera by scanning the nanoprobe on the specimen continuously with a scanning speed of about 10 nm/s.

Isothermal holding at 873K for 1 h led to form a polycrystalline microstructure. Figure 1(a) shows an energy-filtered dark-field image obtained from the annealed specimen. In the image, we can see many bright dots indicating densely formed nanocrystalline grains with sizes of less than 10 nm. To obtain average structural information from the crystallized specimen, we examined a reduced interference function $[Qi(Q)]$ derived from an energy-filtered SAED pattern of the annealed specimen. A procedure for obtaining the $i(Q)$ curve from SAED is referred to the previous paper.[25] The $Qi(Q)]$ profile is shown in Fig. 1(b), together with the corresponding SAED pattern. For comparison, a calculated $Qi(Q)$ profile obtained from the $Fe_{23}B_6$ structure is also shown. Here, $i(Q)$ means the interference function and Q is the scattering vector defined as $Q=4\pi \sin\theta/\lambda$, where θ is the scattering angle and λ the electron wavelength. In the $Qi(Q)$ profile, we see many subpeaks due to the crystallization as well as main peaks. All the peaks and subpeaks for the crystallized specimen can be basically explained from the $Fe_{23}B_6$ structure as was mentioned in the previous work.[26] Only from the $Qi(Q)$ profile, however, it is hard to understand the local structural changes toward a formation of $Fe_{23}B_6$. Next we took many single electron-diffraction patterns (more than 100) from a whole region of the specimen using a NBED technique, in order to examine the structures of local regions.

By using a TV-recording NBED technique, we obtained several types of diffraction patterns from the crystallized specimen annealed at 873K for 1 h. Here we show two types of NBED patterns from perfect $Fe_{23}B_6$ and $Fe_{23}B_6$-like structures [Figs. 2(a) and 2(b)]. For comparison, the calculated NBED pattern of the $Fe_{23}B_6$ structure is shown in Fig. 2(a′). The electron incidence is parallel to the [110] direction. The experimental NBED pattern of Fig. 2(a) is well consistent with the simulated pattern shown in Fig. 2(a′). On the other hand, the NBED pattern of Fig. 2(b) is slightly different from the perfect $Fe_{23}B_6$ pattern. In the pattern of (b), for example, five strong spots marked by arrow heads are clearly seen in the higher scattering angle region. Note that it is difficult to see such strong spots on the opposite side, because of a slight deviation from the zone axis. In addition, a ratio of $|g_2|/|g_1|$ in (a) is $1.50(=|g_{660}|/|g_{440}|)$, whereas a ratio of $|g_4|/|g_3|$ in (b) is about 1.62 which is nearly equal to the golden ratio (1.618). The golden ratio is well known as an important ratio to characterize quasicrystal structures. To understand differences in both the patterns, enlarged patterns of the regions surrounded by squared area in Figs. 2(a) and 2(b) are shown in Figs. 2(c), 2(d), and 2(c′), and 2(d′), respectively. Both of the patterns Figs. 2(c′) and 2(d′) are close to a (partial) pentagonal shape compared with the patterns (c) and (d). From these results, the $Fe_{23}B_6$-like NBED pattern of (b) is partially characterized by the patterns usually obtained from quasicrystal structures.

Characteristic NBED pattern with pseudotenfold symmetry was also obtained from the annealed specimen as shown in Fig. 3. Interestingly, we can see pseudotenfold diffraction patterns with ten strong diffraction spots along concentric

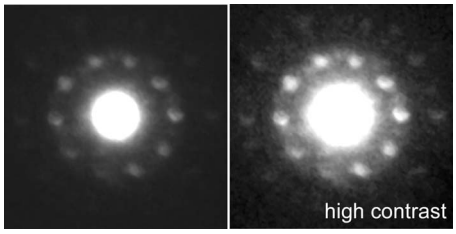

FIG. 3. Pseudotenfold NBED pattern obtained from the specimen annealed at 873K for 1 h. To visualize weak spots in the higher scattering angle region, a high contrasted NBED pattern is also shown in the right side.

circles corresponding to the first and second halo rings of the glass states. Note that distances between neighboring diffraction spots observed on the first halo ring were found to be fluctuated within the range of 6%. Inside a position of the first halo ring (in the lower scattering angle region), we cannot see any strong spot which should be observed in quasicrystal structures. The NBED pattern is quite similar to the pseudotenfold pattern already found in the $Fe_{48}Cr_{15}Mo_{14}C_{15}B_6Tm_2$ BMG.[22]

In this study, we found the quasicrystal-like structure (Fig. 3) as well as the $Fe_{23}B_6$-like intermediate structure between the quasicrystal-like and $Fe_{23}B_6$ crystal structures (Fig. 2). The $Fe_{23}B_6$ structure can be regarded as a crystalline approximant for the quasicrystal-like structure, because of the existence of the $Fe_{23}B_6$-like intermediate structure. It is therefore important to consider how to construct the quasicrystal-like structure based on the $Fe_{23}B_6$ structure including no icosahedral atomic structure as a structural unit. Figure 4(a) shows schematic diagram with an [110] projection of the $Fe_{23}B_6$ structure. A periodic atomic arrangement is seen in the projection, although the arrangement is somewhat complicated. However, we can draw linkages which produce characteristic tiling consisting of deformed pentagons and two types of rhomboids. It was found that these three types of tiles make a deformed decagonal unit as shown in Fig. 4(b) and slight atomic displacements lead to form the exact decagonal unit as shown in Fig. 4(b′). Note that the two types of rhombic tiles found in the unit are just identical to those found in the Penrose tiling. Once we had obtained the three types of tiles, which can make the exact decagonal unit, as shown in Fig. 4(c), we tried to construct a plausible structural model giving the pseudotenfold NBED pattern as shown in Fig. 3. One possible example of the structural model is shown in Fig. 4(d). A space can be filled by the three types of tiles which form the decagonal unit. Interspaces between the decagonal units (indicated by A) can also be filled by the tiles of type 3 [see Fig. 4(c)]. A Fourier transform pattern obtained from the model is shown in the inset of Fig. 4(d). The Fourier transform pattern exhibits a pseudotenfold pattern with no strong spots inside a position of the first halo ring. Note that the strong ten spots were formed just on a position of the first halo ring. The feature of the Fourier transform pattern is similar to that of the experimental NBED pattern as shown in Fig. 3. The high-resolution image observation might reveal atomic arrangements of the quasicrystal-like states. In this stage, however, it

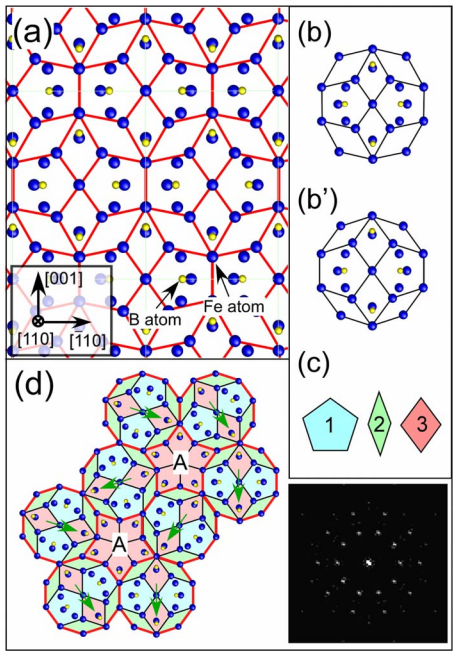

FIG. 4. (Color online) (a) An [110] projection of the $Fe_{23}B_6$ structure. The larger and smaller circles denote the Fe and B atoms, respectively. The linkages between Fe atoms make a tiling with deformed decagonal units. (b) A deformed decagonal unit found in the $Fe_{23}B_6$ structure. (b′) An exact decagonal unit obtained by slight atomic displacements into the deformed unit. (c) Three types of tiles found in the decagonal unit. (d) A preliminary structure model giving the pseudotenfold diffraction pattern, in which the there types of tiles as structural motifs of $Fe_{23}B_6$ are linked each other. A Fourier transform pattern obtained from the model is also shown in the inset. The Fourier transform pattern with ten strong spots is well consistent with the experimental obtained pattern of Fig. 3. Arrows in the model mean orientations of the structural motifs with five different directions, which contribute to give the isotropic diffraction pattern with ten strong spots.

is still difficult to take the image because of the low resolution of the transmission electron microscope (~0.17 nm) and quite small sizes of the grains.

As was mentioned earlier, we already found the quasicrystal-like structure exhibiting pseudotenfold diffraction pattern in the $Fe_{48}Cr_{15}Mo_{14}C_{15}B_6Tm_2$ BMG. It was also found that the quasicrystal-like structure was similar to the χ-FeCrMo structure including icosahedral atomic clusters which are considered to be found in quasicrystals. However, no icosahedral atomic cluster is found in the $Fe_{23}B_6$ structure discussed in the present study. Nevertheless, the pseudotenfold diffraction pattern can be obtained from the quasicrystal-like structure which is linked to the $Fe_{23}B_6$ structure. This is because that the three types of tiles, which can give the decagonal diffraction pattern, was actually found in the $Fe_{23}B_6$ structure as mentioned above. Our finding shows that such an isotropic structure has a close relationship with a glass (or liquid) state, even if icosahedral atomic arrangements are not important in this alloy system.

The quasicrystal-like structure is considered to be related to the medium range ordered (MRO) structure in glass states. This is because strong diffraction spots are found only on a

position of the first halo ring.[26] We actually found that the position of strong NBED spots gradually changes from the halo ring positions to the $Fe_{23}B_6$ positions in the course of the crystallization.[26] Therefore, it is reasonable to consider that the quasicrystal-like structure showing a pseudotenfold NBED pattern (Fig. 3) appears during a change from the glass to crystalline approximant states. In order to elucidate the MRO structure in glass states, it is necessary to understand the local atomic structure of the quasicrystal-like structure. We believe that our viewpoint is one of the important strategies to elucidate the glass structure.

In the course of the nanocrystallization of $Fe_{23}B_6$ in an $(Fe_{0.5}Co_{0.5})_{72}B_{20}Si_4Nb_4$ BMG, we have found a quasicrystal-like structure using a TV-recording NBED technique. The quasicrystal-like structure has a close relationship with the $Fe_{23}B_6$ structure, because the intermediate $Fe_{23}B_6$-like structural state was actually found. The pseudotenfold diffraction patterns from the quasicrystal-like structures in the present alloy probably come from a combination of the three types of tiles found in $Fe_{23}B_6$ where icosahedral atomic arrangements do not exist. This means that the structural motifs without icosahedral atomic arrangements can make up the tenfold quasicrystal-like structure giving a pseudotenfold diffraction pattern. Such an isotropic quasicrystal-like structural state is closely related to the glass (or liquid) state, although including no icosahedral atomic arrangement.

This study was partially supported by Grant-in-Aid for Young Scientists B (Grant No. 20760442) from the Ministry of Education, Culture, Sports, Science and Technology. One of us (A.H.) also acknowledges A. Koreeda for his technical help.

*hirata@wpi-aimr.tohoku.ac.jp

[1] E. Matsubara and Y. Waseda, Mater. Trans., JIM **36**, 883 (1995).
[2] Y. Hirotsu, T. Ohkubo, and M. Matsushita, Microsc. Res. Tech. **40**, 284 (1998).
[3] Y. Waseda, H. S. Chen, K. T. Jacob, and H. Shibata, Sci. Technol. Adv. Mater. **9**, 023003 (2008).
[4] H. W. Sheng, W. K. Luo, F. M. Alamgir, J. M. Bai, and E. Ma, Nature (London) **439**, 419 (2006).
[5] F. C. Frank, Proc. R. Soc. London, Ser. A **215**, 43 (1952).
[6] P. J. Steinhardt, D. R. Nelson, and M. Ronchetti, Phys. Rev. B **28**, 784 (1983).
[7] T. Takagi, T. Ohkubo, Y. Hirotsu, B. S. Murty, K. Hono, and D. Shindo, Appl. Phys. Lett. **79**, 485 (2001).
[8] J. Saida and A. Inoue, J. Non-Cryst. Solids **317**, 97 (2003).
[9] T. Fukunaga, K. Itoh, T. Otomo, K. Mori, M. Sugiyama, H. Kato, M. Hasegawa, A. Hirata, Y. Hirotsu, and A. C. Hannon, Mater. Trans. **48**, 1698 (2007).
[10] X. Hui, H. Z. Fang, G. L. Chen, S. L. Shang, Y. Wang, and Z. K. Liu, Appl. Phys. Lett. **92**, 201913 (2008).
[11] U. Köster, J. Meinhardt, S. Roos, and H. Liebertz, Appl. Phys. Lett. **69**, 179 (1996).
[12] L. Q. Xing, T. C. Hufnagel, J. Eckert, W. Loser, and L. Schultz, Appl. Phys. Lett. **77**, 1970 (2000).
[13] J. Saida, M. Matsushita, and A. Inoue, Appl. Phys. Lett. **79**, 412 (2001).
[14] M. W. Chen, I. Dutta, T. Zhang, A. Inoue, and T. Sakurai, Appl. Phys. Lett. **79**, 42 (2001).
[15] T. Waniuk, J. Schroers, and W. L. Johnson, Phys. Rev. B **67**, 184203 (2003).
[16] K. Kajiwara, M. Ohnuma, T. Ohkubo, D. H. Ping, and K. Hono, Mater. Sci. Eng., A **375-377**, 738 (2004).
[17] C. Li and A. Inoue, Phys. Rev. B **63**, 172201 (2001).
[18] V. Elser and C. L. Henley, Phys. Rev. Lett. **55**, 2883 (1985).
[19] P. H. Gaskell, J. Non-Cryst. Solids **75**, 329 (1985).
[20] M. Imafuku, S. Sato, E. Matsubara, and A. Inoue, J. Non-Cryst. Solids **312-314**, 589 (2002).
[21] Y. Waseda and H. S. Chen, Sci. Rep. Res. Inst. Tohoku Univ. A **28**, 143 (1980).
[22] A. Hirata, Y. Hirotsu, K. Amiya, and A. Inoue, Phys. Rev. B **79**, 020205(R) (2009).
[23] A. Hirata, Y. Hirotsu, K. Amiya, and A. Inoue, Phys. Rev. B **78**, 144205 (2008).
[24] K. Amiya, A. Urata, N. Nishiyama, and A. Inoue, J. Appl. Phys. **97**, 10F913 (2005).
[25] A. Hirata, Y. Hirotsu, T. Ohkubo, T. Hanada, and V. Z. Bengus, Phys. Rev. B **74**, 214206 (2006).
[26] A. Hirata, Y. Hirotsu, K. Amiya, N. Nishiyama, and A. Inoue, Intermetallics **16**, 491 (2008).